THE JOURNAL OF PHYSICAL CHEMISTRY B

Article

pubs.acs.org/JPCB

Stochastic Modeling of Flexible Biomolecules Applied to NMR Relaxation. I. Internal Dynamics of Cyclodextrins: γ-Cyclodextrin as a Case Study

Mirco Zerbetto,[†] Dmytro Kotsyubynskyy,[†] Jozef Kowalewski,[‡] Göran Widmalm,[§] and Antonino Polimeno[†,*]

[†]Dipartimento di Scienze Chimiche, Università degli Studi di Padova, Padova 35131, Italy

[‡]Department of Materials and Environmental Chemistry, Stockholm University, S-106 91 Stockholm, Sweden

[§]Department of Organic Chemistry, Stockholm University, S-106 91 Stockholm, Sweden

Supporting Information

ABSTRACT: In this work, we address the description of the dynamics of cyclodextrins in relation with nuclear magnetic resonance (NMR) relaxation data collected for hydroxymethyl groups. We define an integrated computational approach based on the definition and parametrization of a stochastic equation able to describe the relevant degrees of freedom affecting the NMR observables. The computational protocol merges molecular dynamics simulations and hydrodynamics approaches for the evaluation of most of the molecular parameters entering the stochastic description of the system. We apply the method to the interpretation of the ^{13}C NMR relaxation of the $-CH_2OH$ group of cyclodextrins. We use γ-cyclodextrin as a case study. Results are in agreement with quantitative and qualitative analyses performed in the past with simpler models and molecular dynamics simulations. The element of novelty in our approach is in the treatment of the coupling of the relevant internal (glucopyranose ring twisting/tilting and hydroxymethyl group jumps) and global (molecular tumbling) degrees of freedom.

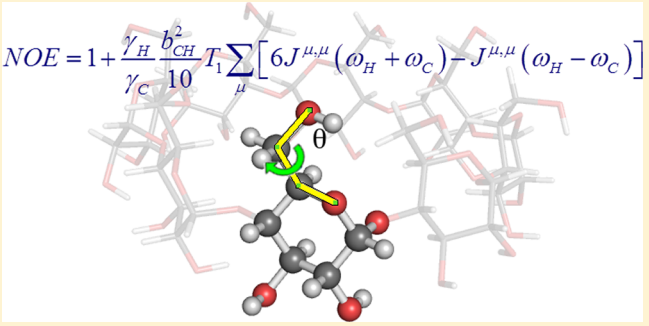

I. INTRODUCTION

Nuclear magnetic resonance (NMR) relaxation measurements are among the most powerful techniques in the investigation of structural and dynamic properties of biomolecules.[1−5] Stochastic methods are appropriate to describe magnetic spectroscopy observables provided that a set of relevant coordinates, supposedly affecting directly the spectroscopic data, can be identified. Within this assumption, which is usually based on the time-scale separation between the relaxation of the set of relevant coordinates and of the remaining degrees of freedom, it is possible to extract useful information on the local mobility of flexible molecules, global reorientation properties and so on. The quality and the extent of information that can be obtained from NMR spectroscopic observables of flexible, even moderately large, molecules is limited since a large computational effort may be required to calculate long enough trajectories in a classical, full-atom (molecular dynamics) simulation to allow a statistically significant evaluation of the time-correlation functions directly linked to the experimental observables. Thus, *ad hoc* modeling based on separate levels of treatment of relevant and nonrelevant sets of coordinates may represent a profitable alternative. Among other possible approaches, methods based on many-body diffusive (Fokker−Planck) modeling of the relevant coordinates have been shown to be effective and versatile.[6−9] In practice, setting-up a stochastic description requires (*i*) an effective mean field expression for the potential energy surface governing the relevant degrees of freedom, and (*ii*) a generalized diffusion/friction matrix, describing the dissipative forces acting on the system. Stochastic models are typically characterized by a huge reduction in dimensionality (and complexity) with respect to a full-atom description, and therefore the computational effort required to calculate correlation functions is greatly decreased.[10] In the past, applications of two-body purely diffusive stochastic models have been presented within the so-called slowly relaxing local structure (SRLS) formalism, which has been largely applied to NMR studies of local dynamics in proteins.[7,9,11−13] More recently, a model based on the dynamics of an internal conformational degree of freedom coupled to global reorientation has been presented for the study of oligosaccharides.[8]

We address in this paper the interpretation of NMR relaxation data of cyclodextrins, based on a stochastic approach. Cyclodextrins, particularly the common α-, β-, and γ-cyclo-

Received: July 4, 2012
Revised: October 11, 2012
Published: October 11, 2012

dextrins are made of a limited number of α-(1→4)-linked glucopyranose units forming ring structures. Cyclodextrins possess some unique properties, such as efficient inclusion complexation of small molecules inside the molecular cavity. These properties require the existence of some mobility of the glucose units, but motions of particular pyranose rings are restricted by virtue of the cyclic structure of the cyclodextrins. It is thus of practical interest to study and possibly predict mobility properties of cyclodextrins and similar compounds.

As a case study, we consider here the well-known example of γ-cyclodextrin NMR relaxation data. We employ previously published ^{13}C relaxation data for hydroxymethyl group[14] including cross-correlated relaxation rates (CCRR). A molecular description of the internal dynamics of γ-cyclodextrin is quite challenging because, at least in principle, suitable generalized coordinates should be introduced to describe the motion of the closed ring formed by the α-glucopyranose units. Several attempts in understanding internal dynamics using NMR spectroscopy were reported in the past. Kowalewski and Widmalm[15] fitted multifield relaxation data obtained for ring carbons using the Lipari−Szabo approach.[16,17] Ghalebani et al.[14] studied the dynamics of hydroxymethyl groups, fitting multifield relaxation data to the two-site jump model.[18] In a recent paper Bernatowicz et al.[19] applied a discrete multisite local dynamics formalism[20] to the relaxation data of the ring carbons.

We adopt here an extended version of the SRLS method that takes into account, as internal coordinates, both the twisting/tilting of the glucopyranose unit and the jump motion of the hydroxymethyl group between two conformations. The latter motion has been experimentally confirmed to occur on a time scale that can sensibly affect NMR relaxation.[21,22]

An integrated computational protocol for the partial parametrization of the model is employed by combining *ad hoc* tools for the evaluation of the required molecular parameters. We therefore employ molecular dynamics (MD) and hydrodynamics (HD) approaches to evaluate most of the required molecular properties and merge this information into the definition of the basic stochastic equation that is then solved to calculate the required observables. Such strategy has been applied by some of us already to NMR relaxation studies.[8,9] Even if an exhaustive definition of all the parameters entering the model is not possible (see below), the number of remaining free parameters is greatly reduced and the requirement of fitting procedures is kept to a minimum.

This paper is organized as follows. In section II, a brief, but complete theoretical and computational background is provided, and the extended SRLS model is presented and discussed; in section III, the model is applied to the interpretation of NMR relaxation data of γ-cyclodextrin. In section IV, a short discussion of the results is provided.

II. THEORETICAL AND COMPUTATIONAL BACKGROUND

II.A. Modeling. The SRLS[10] model is extended here by including an internal coordinate describing the jump motion of the hydroxymethyl group between two conformations. We call this model the two-state slowly relaxing local structure (TS-SRLS) model.

In the standard SRLS model, the relevant dynamics of the molecule is associated with two rigid rotators reorienting in a medium, coupled by a potential of mean torque. The model was first introduced by Polimeno and Freed[10] for interpreting continuous wave electron spin resonance (cw-ESR) spectra line-shapes of small rigid paramagnetic probes in ordered media (liquid crystals, glasses). The SRLS model has been successively applied to the interpretation of ESR and NMR spectroscopic observables in proteins and biomolecules.[7,9,11,12,23] In this context the two "bodies" assume a slightly different interpretation with respect to the original SRLS model. In particular the first body (the slowest one, in terms of correlation time) represents the global reorientation of the whole molecule, while the second one collects all the local motions in the proximity of the part of the molecule bearing the probe (e.g., the local motions making one amino acid reorienting with respect to the whole protein in interpreting NMR relaxation of proteins). The coupling potential mimics the motional restrictions of the second body with respect to the first one due to the chemical bonds. The effect of the coupling between the two bodies is expected to be important in the application to cyclodextrins and a short discussion on the effect of decoupling is provided in the Supporting Information.

For the interpretation of NMR relaxation data of cyclodextrins we augment the standard SRLS model by introducing a further internal degree of freedom describing the jump motion of the hydroxymethyl group. Thus, the TS-SRLS is, formally, a three-body model. The first body represents the global tumbling of the molecule; the second body describes the internal motions that make one sugar ring tilt and twist with respect to the entire molecule. Finally, the third body is the hydroxymethyl group that can change orientation on the glucopyranose unit. The full set of stochastic coordinates is then $Q = (X, \theta)$, where $X = (\Omega_{LF\text{-}VF}, \Omega_{LF\text{-}OF})$, being that $\Omega_{LF\text{-}VF}$ and $\Omega_{LF\text{-}OF}$ are the two sets of Euler angles defining the rotation from a laboratory frame (LF) to two frames fixed, respectively, on the first and second bodies, VF and OF (see Figure 1); θ is the torsional angle shown in Figure 2, describing a change in the orientation of the hydroxymethyl group on the sugar ring. The Smoluchowski equation giving the time evolution of the conditional probability density of finding the system in

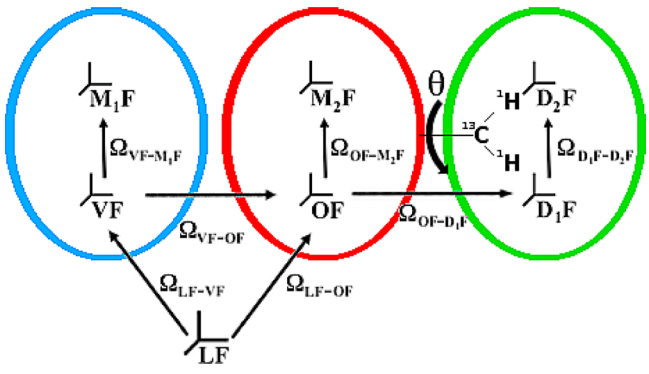

Figure 1. Reference frames defining the TS-SRLS model adapted to the $^{13}C^{1}H_2$ probe. The first body is represented by the blue ellipse on the left, the second body is the red ellipse on the right, bearing the magnetic probe. LF is the laboratory frame; VF and M_1F are, respectively, the local director and global diffusion frames, fixed on the first body; OF and M_2F are, respectively, the local ordering and local diffusion frames, fixed on the second body; D_1F and D_2F are the two $^{13}C-^{1}H$ dipolar magnetic frames, fixed on the second body. The sets of Euler angles corresponding to the respective frame transformations are also depicted. The sets $\Omega_{LF\text{-}VF}$, $\Omega_{LF\text{-}OF}$, and $\Omega_{VF\text{-}OF}$ are time-dependent. In the TS-SRLS model, the Euler angles $\Omega_{OF\text{-}D1F}$ are also time-dependent.

dx.doi.org/10.1021/jp306624d | J. Phys. Chem. B 2012, 116, 13159−13171

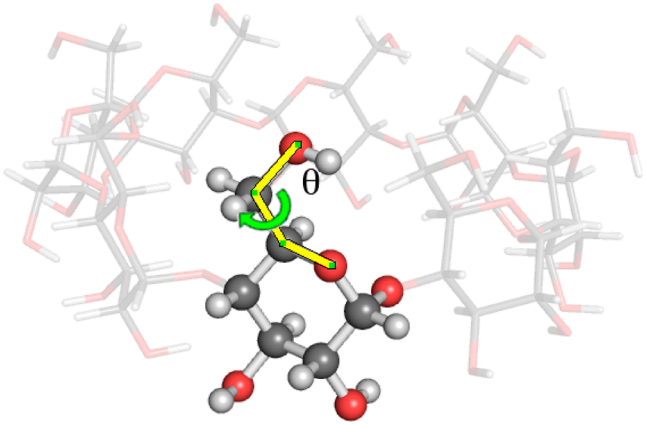

Figure 2. Definition of the θ torsional angle on the α-glucopyranose unit of the γ-cyclodextrin describing the rotation of the hydroxymethyl group with respect to the sugar ring.

configuration $\mathbf{Q}$ at time t, if it was at some starting point $\mathbf{Q}_0$ at t_0, $P(\mathbf{Q},t|\mathbf{Q}_0,t_0)$, takes the form

$$\frac{\partial P(\mathbf{Q}, t|\mathbf{Q}_0, t_0)}{\partial t} = -\hat{\Gamma}(\mathbf{Q})P(\mathbf{Q}, t|\mathbf{Q}_0, t_0) = -\hat{\Gamma}_{SRLS}(\mathbf{X})P(\mathbf{Q}, t|\mathbf{Q}_0, t_0) + \hat{\Gamma}_{RW}(\mathbf{Q})P(\mathbf{Q}, t|\mathbf{Q}_0, t_0) \quad (1)$$

where $\hat{\Gamma}_{SRLS}(\mathbf{X})$ is the standard SRLS Smoluchowski operator and $\hat{\Gamma}_{RW}(\mathbf{Q})$ is the random walk operator describing the motion of the hydroxymethyl group. The former is usually defined as[10]

$$\hat{\Gamma}_{SRLS}(\mathbf{X}) = -\begin{bmatrix} \hat{\mathbf{J}}_1(\Omega_{\text{LF-VF}}) \\ \hat{\mathbf{J}}_2(\Omega_{\text{LF-OF}}) \end{bmatrix}^t \begin{bmatrix} \mathbf{D}_1 & \mathbf{0} \\ \mathbf{0} & \mathbf{D}_2 \end{bmatrix} P_{eq}(\mathbf{X}) \begin{bmatrix} \hat{\mathbf{J}}_1(\Omega_{\text{LF-OF}}) \\ \hat{\mathbf{J}}_2(\Omega_{\text{LF-OF}}) \end{bmatrix} P_{eq}^{-1}(\mathbf{X}) \quad (2)$$

where $\hat{\mathbf{J}}_i$ and $\boldsymbol{D}_i$ are respectively the angular momentum operator acting on the ith body and the ith body rotational diffusion tensor; no hydrodynamic coupling between the bodies is assumed (null out-of-diagonal blocks of the full diffusion tensor) and the Boltzmann equilibrium distribution is assumed as $t \to \infty$

$$P_{eq}(\mathbf{X}) = \exp[-U(\mathbf{X})/k_BT]/\langle\exp[-U(\mathbf{X})/k_BT]\rangle \quad (3)$$

where $U(\boldsymbol{X})$ is the coupling potential, k_B the Boltzmann constant and T the absolute temperature. A simple shape is assumed for the potential, defined as the combination of only Wigner matrices of rank 2. The two frames fixed on the bodies are chosen such that VF represents the local director frame and OF represents the local ordering frame (OF). Moreover, even if the stochastic process $\boldsymbol{X}$ has a trivial interpretation, it is more convenient to transform to the process $\boldsymbol{Y} = (\Omega_{\text{LF-VF}},\Omega_{\text{VF-OF}})$, where $\Omega_{\text{VF-OF}} = \Omega_{\text{LF-OF}} - \Omega_{\text{LF-VF}}$ is the set of Euler angles giving the relative orientation of the two bodies. Here, the coupling potential spanned over rank 2 Wigner matrices, in case of isotropic medium, takes the simple form[24]

$$U(\mathbf{Y})/k_BT = -c_0^2 D_{0,0}^2(\Omega_{\text{VF-OF}}) - c_2^2[D_{0,2}^2(\Omega_{\text{VF-OF}}) + D_{0,-2}^2(\Omega_{\text{VF-OF}})] \quad (4)$$

where $D^J_{M,K}(\Omega)$ is a Wigner matrix and only two real dimensionless coefficients, c_0^2 and c_2^2, parametrize the potential. Details of the definition and implementation of this model can be found elsewhere.[10]

The random walk operator, $\hat{\Gamma}_{RW}(\mathbf{Q})$, is defined by the following master equation

$$\hat{\Gamma}_{RW}P(\mathbf{Q}, t) = \int d\mathbf{Q}'[P(\mathbf{Q}, t)W(\mathbf{Q} \to \mathbf{Q}') - P(\mathbf{Q}', t)W(\mathbf{Q}' \to \mathbf{Q})] \quad (5)$$

where from now on $\boldsymbol{Q} = (\boldsymbol{Y},\theta)$ and we omitted the conditional dependence of the probability density on the initial state; i.e., from now on we shall use $P(\mathbf{Q},t) \equiv P(\mathbf{Q},t|\mathbf{Q}_0,t_0)$. We model the kernel of the transformation, $W(\mathbf{Q}\to\mathbf{Q}')$, assuming that (i) a change in the internal coordinate variable θ does not influence the orientation of the two bodies, (ii) the equilibrium distribution of θ is independent of the other coordinates, i.e., $P_{eq}(\mathbf{Q}) = P_{eq}(\boldsymbol{Y})P_{eq}(\theta)$, and (iii) the frequency, ω_R, of the jumps among sites is independent of the configuration

$$W(\mathbf{Q} \to \mathbf{Q}') = \omega_R\delta(\Omega_{\text{LF-VF}} - \Omega'_{\text{LF-VF}})\delta(\Omega_{\text{VF-OF}} - \Omega'_{\text{VF-OF}})P_{eq}(\theta') \quad (6)$$

By substituting this kernel into eq 5, introducing the symmetrization of the Smoluchowski operator, $\tilde{\Gamma} = P_{eq}^{-1/2}(\mathbf{Q})\hat{\Gamma}P_{eq}^{1/2}(\mathbf{Q})$, and the symmetrized probability density $\tilde{P}(\mathbf{Q}, t) = P_{eq}^{-1/2}(\mathbf{Q})P(\mathbf{Q}, t)$ the random walk operator reads

$$\tilde{\Gamma}_{RW}\tilde{P}(\mathbf{Q}, t) = \omega_R[1 - P_{eq}^{1/2}(\theta)\int dq'\, P_{eq}^{1/2}(\theta')\cdot]\tilde{P}(\mathbf{Q}, t) \quad (7)$$

The latter equation is quite general. We shall take into account that the jump motion occurs between only two discrete states, which we label θ_1 and θ_2. The assumption of two, rather than three discrete states is supported by the fact that a 1,3-diaxial interaction between C4−O4 and C6−O6 is highly unfavorable.[25] Thus, the random walk operator defined in eq 7 can be recast into the following discrete form

$$\tilde{\Gamma}_{RW} = \omega_R - \omega_R[\rho_1^{1/2}\delta(\theta - \theta_1) + \rho_2^{1/2}\delta(\theta - \theta_2)] \sum_{\theta'}[\rho_1^{1/2}\delta(\theta' - \theta_1) + \rho_2^{1/2}\delta(\theta' - \theta_2)]\cdot \quad (8)$$

where we introduced the notation $\rho_i = P_{eq}(\theta)_{|\theta=\theta_i}$. Because the constraint $\rho_1 + \rho_2 = 1$ holds, the introduction of the internal coordinate θ adds two more ingredients to the problem, namely the jumping frequency, ω_R, and the population of one of the two states. We report in Appendix A the detailed description of the random walk operator and how the calculation of spectral densities is changed with respect to the standard SRLS model.

In the TS-SRLS model we are explicitly not including the hydroxymethyl group H−C−H fast libration because it is reasonable to assume that such a fast, small-amplitude motion has a negligible effect on the dynamics of the system. However, vibrational averaging of NMR observables has an important effect on the "observed" H−C−H bond angle. Thus, for the sake of completeness we show in Appendix B how the H−C−H libration can be included and how its effect on NMR data

dx.doi.org/10.1021/jp306624d | J. Phys. Chem. B 2012, 116, 13159−13171

and model parameters estimation can be evaluated within a number of reasonable approximations.

To fully parametrize the TS-SRLS model one needs at least the two diffusion tensors (principal values and orientation on the bodies), the two coefficients of the potential, the population of one of the two states and the jumping frequency. Thus, the complete set of parameters amounts to a total of 16 numbers. Moreover, other geometrical quantities will enter the description increasing the complexity of the input of the model. In particular, for the $^{13}C^{1}H_2$ magnetic probe, we need in addition the orientation of the dipolar interaction frame (three angles *per* frame), the C−H bond length, and the H−C−H bond angle. It is unthinkable to obtain all these parameters from a fitting procedure. Thus, we set up an integrated computational protocol able to supply the greater possible number of model parameters. In particular we could evaluate the global diffusion tensor, the coefficients of the potential in eq 4, the population of the two minima for the hydroxymethyl jump motion.

To evaluate the global rotational diffusion tensor of the molecule (first body) we employ a hydrodynamics (HD) based approach, which has shown to be reliable for the calculation of the rotational diffusion tensor of molecules of different sizes.[26−28] The molecule is pictured as a set of constrained spheres, where constraints arise from chemical bonds. The procedure consists in the calculation of the friction tensor of the unconstrained spheres followed by the application of a geometric matrix of constraints to recover the generalized friction tensor of the object.[28−30] It is straightforward to take into account flexible molecules.[28]

We use molecular dynamics (MD) simulations to evaluate the two potential coefficients, c_0^2 and c_2^2, in eq 4. We follow closely the protocol described at length in ref9 and we give here only a short summary of the method. First, the MD trajectory is referred, by means of a roto-translation, to a molecule-fixed reference frame. We take the principal inertia frame for convenience. Second, a k-clustering of the trajectory is performed and the snapshot closest to the center of the most populated cluster is selected as the reference structure. This is thought to be the molecular conformation for which the potential of mean force is in its minimum. Using this reference configuration, and considering the properties of the potential defined in eq 4, it is possible to define the orientation of the two frames, VF and OF, with respect to selected atoms among those belonging to the probe (second body). Third, using the geometrical information obtained in the previous step, the time series of the $\Omega_{\text{VF-OF}}$ set of Euler angles is extracted from the trajectory. This time series gives access to the (diagonal) order tensor, the spherical components of which are $S_0^2 = \langle D_{0,0}^2(\Omega_{\text{VF-OF}})\rangle$ and $S_2^2 = \langle D_{0,2}^2(\Omega_{\text{VF-OF}}) + D_{0,-2}^2(\Omega_{\text{VF-OF}})\rangle$, where $\langle ...\rangle$ means averaging over the sample. The explicit parametric dependence of the order parameters on the coefficients of the potential is

$$S_k^2(c_0^2, c_2^2) = \left[\int d\Omega_{\text{VF-OF}} \left[D_{0,k}^2(\Omega_{\text{VF-OF}}) + D_{0,-k}^2(\Omega_{\text{VF-OF}})\right] e^{c_0^2 D_{0,0}^2(\Omega_{\text{VF-OF}}) + c_2^2[D_{0,2}^2(\Omega_{\text{VF-OF}}) + D_{0,-2}^2(\Omega_{\text{VF-OF}})]}\right] / \left[(1+\delta_{k,0})\int d\Omega_{\text{VF-OF}} e^{c_0^2 D_{0,0}^2(\Omega_{\text{VF-OF}}) + c_2^2[D_{0,2}^2(\Omega_{\text{VF-OF}}) + D_{0,-2}^2(\Omega_{\text{VF-OF}})]}\right] \quad (9)$$

with $k = 0, 2$. Thus, once the order parameters are known from the MD simulation, the coefficients of the potential, c_0^2 and c_2^2, can be evaluated solving a nonlinear system of equations.[9]

The populations of the two states describing the orientation of the hydroxymethyl group on the α-glucopyranose unit have been obtained from the histogram analysis of the time series of the θ torsion angle extracted from the MD trajectory. We select ρ_1 and ρ_2 such that their ratio is the same as that obtained from the probability density values of two peaks in the histogram (see section III).

Here we are taking into consideration the $^{13}C^{1}H_2$ probes for which the chemical shift anisotropy contribution is usually neglected[31] and only the dipolar magnetic interaction is taken into account. To parametrize the dipolar contribution to the spin relaxation one needs some geometric parameters and in particular the C−H bond length, the H−C−H angle, and the set of Euler angles giving the orientation of the frame (DF) that diagonalizes the dipolar interaction. This frame has the *Z*-axis along the C−H bond while the orientation of the other two axes does not influence the results because the dipolar tensor is axially symmetric. This set of data can be obtained from the molecular structure.

What is left is the evaluation of the local diffusion tensor (i.e., the rotational diffusion tensor of the second body) and the jumping frequency. The local diffusion tensor has a quite complicated molecular definition and hydrodynamics arguments cannot be generally employed. For these reasons, at present, an efficient evaluation procedure for this parameter is not yet available. Thus, the principal values and the orientation of the local diffusion tensor on the probe are taken as free parameters and are determined via a nonlinear least-squares fitting procedure. We introduce a reasonable simplification of the physical picture by choosing the local diffusion tensor to be an axially symmetric tensor. This assumption still preserves a good level of complexity/adaptability of the model, but limits the number of free parameters. Finally, the jumping frequency is also treated as a free parameter. Thus, 5 out of 24 parameters are fitted, namely: two diffusion rates for local motion, two spherical angles giving the orientation of the tensor on the probe, and the jumping frequency. These parameters will be evaluated by means of a nonlinear least-squares fitting procedure.

II.B. Evaluation of NMR Observables. We are interested here in molecules diffusing in low viscosity media such that molecular motions relax in time scales much faster with respect to the spin relaxation processes. Thus, the dynamics of the systems that we are studying falls within the Redfield limit. Following basic theory of spin relaxation[32] and making use of the theory of linear responses the NMR relaxation data are evaluated directly from the spectral densities of the auto- and cross-correlation functions of magnetic interactions. Since the CSA contribution for $^{13}C^{1}H_2$ probes can be neglected[31] only the dipolar terms enter in the expressions for the relaxation

dx.doi.org/10.1021/jp306624d | J. Phys. Chem. B 2012, 116, 13159−13171

data. In particular we are interested in the calculation of T_1, T_2, NOE, and the longitudinal and spin-lock dipolar cross-correlated relaxation rates (CCRRs). The explicit expressions are

$$\frac{1}{T_1} = \frac{{b_{CH}}^2}{10}\sum_{\mu}[J^{\mu,\mu}(\omega_H - \omega_C) + 3J^{\mu,\mu}(\omega_C) + 6J^{\mu,\mu}(\omega_H + \omega_C)] \quad (10)$$

$$\frac{1}{T_2} = \frac{{b_{CH}}^2}{20}\sum_{\mu}[4J^{\mu,\mu}(0) + J^{\mu,\mu}(\omega_H - \omega_C) + 3J^{\mu,\mu}(\omega_C) + 6J^{\mu,\mu}(\omega_H) + 6J^{\mu,\mu}(\omega_H + \omega_C)] \quad (11)$$

$$NOE = 1 + \frac{\gamma_H}{\gamma_C}\frac{{b_{CH}}^2}{10}T_1\sum_{\mu}[6J^{\mu,\mu}(\omega_H + \omega_C) - J^{\mu,\mu}(\omega_H - \omega_C)] \quad (12)$$

$$\Gamma_{\text{long}} = \frac{3}{5}{b_{CH}}^2 J^{1,2}(\omega_C) \quad (13)$$

$$\Gamma_{\text{spin-lock}} = \frac{3}{10}{b_{CH}}^2\left[\frac{4}{3}J^{1,2}(0) + J^{1,2}(\omega_C)\right] \quad (14)$$

where $J^{\mu,\nu}$ is the dipole−dipole auto- ($\mu = \nu$) or cross- ($\mu \neq \nu$) correlated spectral density, $b_{CH} = \mu_0\gamma_H\gamma_C\hbar/4\pi{r_{CH}}^3$, γ_X and ω_X are, respectively, the magnetogyric ratio and the Larmor frequency of nucleus X, and r_{CH} is the C−H bond length. The summation index in eqs 10−12 runs over the hydrogen nuclei bonded to the ^{13}C atom.

All the spectral densities in the previous equations are obtained as Fourier−Laplace transforms of the normalized time correlation functions

$$J^{\mu,\nu}(\omega) = \frac{\int_0^\infty \mathrm{d}t\, e^{-i\omega t}\langle D^J_{M,0}[\Omega_{L\mu}(0)]^* D^J_{M,0}[\Omega_{L\nu}(t)]\rangle}{\langle D^J_{M,0}[\Omega_{L\mu}(0)]^* D^J_{M,0}[\Omega_{L\nu}(0)]\rangle} \quad (15)$$

where $\Omega_{L\mu}(t)$ is the stochastic set of Euler angles transforming from the laboratory frame, LF, to the principal axes frame of the μth magnetic tensor, μF. Equation 15 holds in the secular approximation. Because the magnetic interactions in which we are interested are represented by symmetric and traceless rank 2 tensors, only terms with $J = 2$ are preserved. Furthermore, due to the isotropy of the medium, we set $M = 0$.

We recall that in the standard SRLS model the static purely geometric contribution of the magnetic part and the contribution of the dynamics of the system can be split in eq 15 by using the fact that $\Omega_{L\mu}(t) = \Omega_{\text{OF-}\mu\text{F}} + \Omega_{\text{LF-OF}}(t)$, i.e., the orientation of the magnetic tensor with respect to LF is divided into a stochastic set of Euler angles, $\Omega_{\text{LF-OF}}(t)$ and a time-independent rotation over the probe, $\Omega_{\text{OF-}\mu\text{F}}$, transforming from OF to μF. Given this combined set of rotations and using the properties of Wigner matrices in eq 15 we obtain

$$J^{\mu,\nu}(\omega) = \frac{1}{5}\sum_{K,K'=-2}^{2} {D_{K,0}}^2(\Omega_{\text{OF-}\mu\text{F}})^* {D_{K',0}}^2(\Omega_{\text{OF-}\nu\text{F}}) \times \int_0^\infty \mathrm{d}t\; e^{-i\omega t}\langle {D_{0,K}}^2[\Omega_{\text{LF-OF}}(0)]^* {D_{0,K'}}^2[\Omega_{\text{LF-OF}}(t)]\rangle = \frac{1}{5}\sum_{K,K'=-2}^{2} {D_{K,0}}^2(\Omega_{\text{OF-}\mu\text{F}})^* {D_{K',0}}^2(\Omega_{\text{OF-}\nu\text{F}})\, j_{K,K'}(\omega) \quad (16)$$

When eq 16 holds (i.e., when $\Omega_{\text{OF-}\mu\text{F}}$ can be taken time-independent), it represents a general equation to bridge between molecular details and NMR data. The details, in terms of structure and dynamics, are contained in the reduced spectral densities $j_{K,K'}(\omega)$, which are the only quantities being modified if the model for the dynamics is changed. In the SRLS model, the reduced spectral densities are calculated taking into account that $\Omega_{\text{LF-OF}}(t)$ is a combination of two stochastic rotations, the former transforming from the LF to VF, and the second rotation transforming from VF to OF. Details of the implementation can be found elsewhere.[33,34] In the TS-SRLS model, however, eq 16 is not valid because $\Omega_{\text{OF-}\mu\text{F}} = \Omega_{\text{OF-}\mu\text{F}}(\theta)$ is a stochastic set of Euler angles. With some work, it is possible to find an expression analogous to eq 16, i.e.

$$J^{\mu,\nu}(\omega) = \sum_{K,K'}\mathrm{Re}\{\chi^{+*}_{\mu,K}\chi^{+}_{\nu,K'}\}j^{+}_{K,K'}(\omega) + \mathrm{Re}\{\chi^{-*}_{\mu,K}\chi^{-}_{\nu,K'}\}\, j^{-}_{K,K'}(\omega) \quad (17)$$

where

$$\chi^{+}_{\mu,K} = \rho_1 {D_{K,0}}^2(\Omega_{\mu,1}) + \rho_2 {D_{K,0}}^2(\Omega_{\mu,2}) \quad (18)$$

$$\chi^{-}_{\mu,K} = \sqrt{\rho_1\rho_2}\,{D_{K,0}}^2(\Omega_{\mu,1}) - \sqrt{\rho_1\rho_2}\,{D_{K,0}}^2(\Omega_{\mu,2}) \quad (19)$$

and $\Omega_{\mu,i} = \Omega_{\text{OF-}\mu\text{F}}(\theta)_{|\theta=\theta_i}$. The $j^{+}_{K,K'}(\omega)$ functions correspond exactly to the SRLS reduced spectral densities appearing in the last equality of eq 16, while the $j^{-}_{K,K'}(\omega)$ functions are the same spectral densities but calculated with an intrinsic line width corresponding to ω_R. The detailed derivation of eq 17 is reported in Appendix A.

II.C. Numerical Solution. Because of the low dimensionality of the system we can search for the numerically exact solution of the Smoluchowski equation, at a moderate computational cost. For this purpose we follow a standard method based on the projection of the diffusive operator on a set of orthonormal basis functions. We use the direct product basis set given by $|\Lambda\rangle = |\lambda\rangle \otimes |n\rangle = |L_1M_1K_1\rangle \otimes |L_2M_2K_2\rangle \otimes |n\rangle$, where

$$|L_1M_1K_1\rangle = \sqrt{\frac{2L_1+1}{8\pi^2}}D^{L_1}_{M_1,K_1}(\Omega_{\text{LF-VF}})$$

$$|L_2M_2K_2\rangle = \sqrt{\frac{2L_2+1}{8\pi^2}}D^{L_2}_{M_2,K_2}(\Omega_{\text{VF-OF}})$$

$$|n\rangle = \delta(\theta - \theta_n) \quad (20)$$

Using the closure relation for the basis set $|\Lambda\rangle$ the reduced spectral densities can be rewritten in matrix form as

$$j_{K,K'}(\omega) = \mathbf{v}^{tr}_K(i\omega\mathbf{1} - \Gamma)^{-1}\mathbf{v}_{K'} \quad (21)$$

dx.doi.org/10.1021/jp306624d | J. Phys. Chem. B 2012, 116, 13159−13171

where:

$$(\Gamma)_{i,j} = \langle \Lambda_i | \tilde{\Gamma} | \Lambda_j \rangle$$

$$(\mathbf{v}_K)_i = \langle \Lambda_i | {D_{0,K}}^2(\Omega) {P_{eq}}^{1/2}(\Omega) \rangle \quad (22)$$

Introducing proper linear combinations of the Wigner matrices ${D_{0,K}}^2(\Omega)$ it is possible to obtain a symmetrized version of eq 21, which allows implementing a simpler and optimized algorithm

$$j^S_{K,K'}(\omega) = \mathbf{v}^S_{K,K'} \cdot (i\omega \mathbf{1} - \Gamma)^{-1} \cdot \mathbf{v}^S_{K,K'} \quad (23)$$

where $\mathbf{v}^S_{K,K'}$ are linear combinations of $\mathbf{v}_K$ and $\mathbf{v}_{K'}$ arrays. Readers interested in mathematical and implementation details are referred to the basic papers on the methods.[6,8,10,33] To solve eq 23 we employ the Lanczos tridiagonalization.[30,35] It is an iterative algorithm creating at every step, n, a tridiagonal symmetric matrix, $\boldsymbol{T}_n$ that approximates the matrix representation of the Smoluchowski operator, Γ, in the sense that the eigenvalues of $\boldsymbol{T}_n$ are the most important eigenvalues of Γ with respect to the physical observable (or starting vector, $\mathbf{v}^S_{K,K'}$). The transformation between the approximate and exact matrices is carried out by the orthonormal matrix $\boldsymbol{Q}_n$, as $\mathbf{T}_n = \mathbf{Q}_n^{tr} \mathbf{\Gamma} \mathbf{Q}_n$. Thus, at any given iteration step n, the approximant $j^S_{K,K',n}(\omega)$ to $j^S_{K,K'}(\omega)$ is given by

$$j^S_{K,K',n}(\omega) = (\mathbf{Q}_n \mathbf{v}^S_{K,K'})^{tr} (i\omega \mathbf{1}_n + \mathbf{T}_n)^{-1} (\mathbf{Q}_n \mathbf{v}^S_{K,K'}) \quad (24)$$

$\mathbf{1}_n$ is the $n \times n$ identity matrix. Using the orthonormality of $\boldsymbol{Q}_n$ the last equation reduces to

$$j^S_{K,K',n}(\omega) = (i\omega \mathbf{1}_n + \mathbf{T}_n)_{1,1}^{-1} \quad (25)$$

i.e., the nth approximant to the reduced spectral density is the (1,1) element of the inverse of the matrix $(i\omega \mathbf{1}_n + \boldsymbol{T}_n)$. Moreover, $j^S_{K,K',n}(\omega)$ can be expressed as a continued fraction:[30,35]

$$j^S_{K,K',n}(\omega) = \cfrac{1}{\alpha_1 - i\omega - \cfrac{{\beta_1}^2}{\alpha_2 - i\omega - \cfrac{{\beta_2}^2}{\alpha_3 - i\omega - \ldots}}} \quad (26)$$

α is the n-dimensional array containing the diagonal elements of $\boldsymbol{T}_n$, and β is the $(n-1)$-dimensional array containing the subdiagonal elements of the tridiagonal (symmetric) matrix.

The whole procedure briefly discussed here is implemented in the C^{2+}OPPS software package developed by some of us,[33,34] which is available to download under the GPL v2 license at the URL http://www.chimica.unipd.it/licc/software.html.

III. CASE STUDY: γ-CYCLODEXTRIN

The initial structure of γ-cyclodextrin was taken from the protein data bank entry 1D3C (X-ray structure of Michaelis complex of *Bacillus circulans* strain 251 cyclodextrin glycosyltransferase with γ-cyclodextrin), residues 700−707. We used NAMD[36] to carry out the molecular dynamics simulations. The carbohydrate solution force field (CSFF)[37] was used for γ-cyclodextrin, and TIP3P force field for water molecules. Two trajectories of 200 ns each were produced after energy minimization, heating and an equilibration period of 1 ns. The full set of parameters of the MD trajectory is reported in Table 1.

We used the CHARMM package[38] to analyze the MD trajectories in order to extract the local potential of mean force

Table 1. MD Simulation Parameters Associated with the Calculation of the Two MD Trajectories for the γ-Cyclodextrin

protein data bank file	1D3C
molecular charge	0
number of water molecules	731
water molecule model	TIP3P
periodic box dimensions	31.432 × 31.808 × 27.492 Å^3
ensemble	N (2361 atoms), P (1 atm), T (300 K)
thermostat	temperature coupling
barostat	Nosé−Hoover Langevin piston (piston period 200 fs, piston decay 100 fs, piston temperature 300 K)
nonbonded interactions cutoff	12 Å, smoothing switch at 10 Å
pair list distance	13.5 Å
electrostatics	PME
time step of integration	2 fs
coordinates and velocities saving frequency	2500 MD steps
equilibration period	1 ns
production period	200 ns

using the protocol summarized in section II.A After referring the trajectory to the principal inertia frame we performed a k-clustering of the MD snapshots based on (φ,ψ) torsional angles indicated in Figure 3, with a maximum root-mean-square cutoff

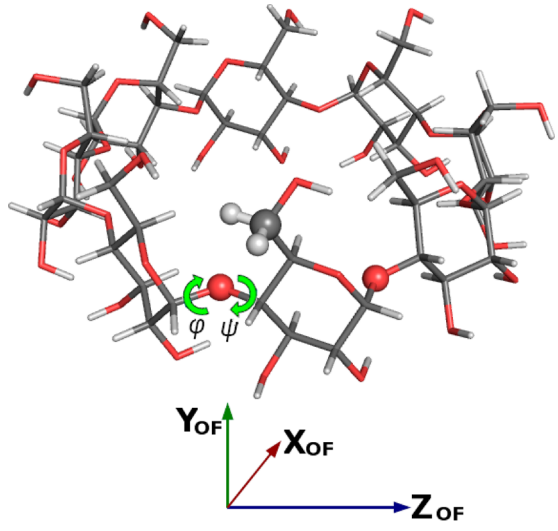

Figure 3. Reference structure of γ-cyclodextrin obtained from MD simulations. The $^{13}C^1H_2$ group is shown in ball-and-stick convention. Torsion angles (φ,ψ) are those responsible for the motion of the α-glucopyranose unit with respect to the molecule. The OF frame is reported below the molecule; the Z-axis is parallel to the axis defined by the glycosidic oxygen atoms highlighted as spheres and the Y-axis is parallel to the principal axis of the cyclodextrin.

of 20 deg. The most probable structure, i.e. the snapshot closest to the center of the most populated cluster, was used to evaluate the relative orientation between the two bodies.[9] We obtained the two order parameters ${S_0}^2 = -0.47$, and ${S_2}^2 = -1.00$, indicating very high ordering, and that correspond to the potential coefficients ${c_0}^2 = -14.24$ and ${c_2}^2 = -2.81$, expressed in k_BT units for $T = 300$ K. Because NMR data were

dx.doi.org/10.1021/jp306624d | J. Phys. Chem. B 2012, 116, 13159−13171

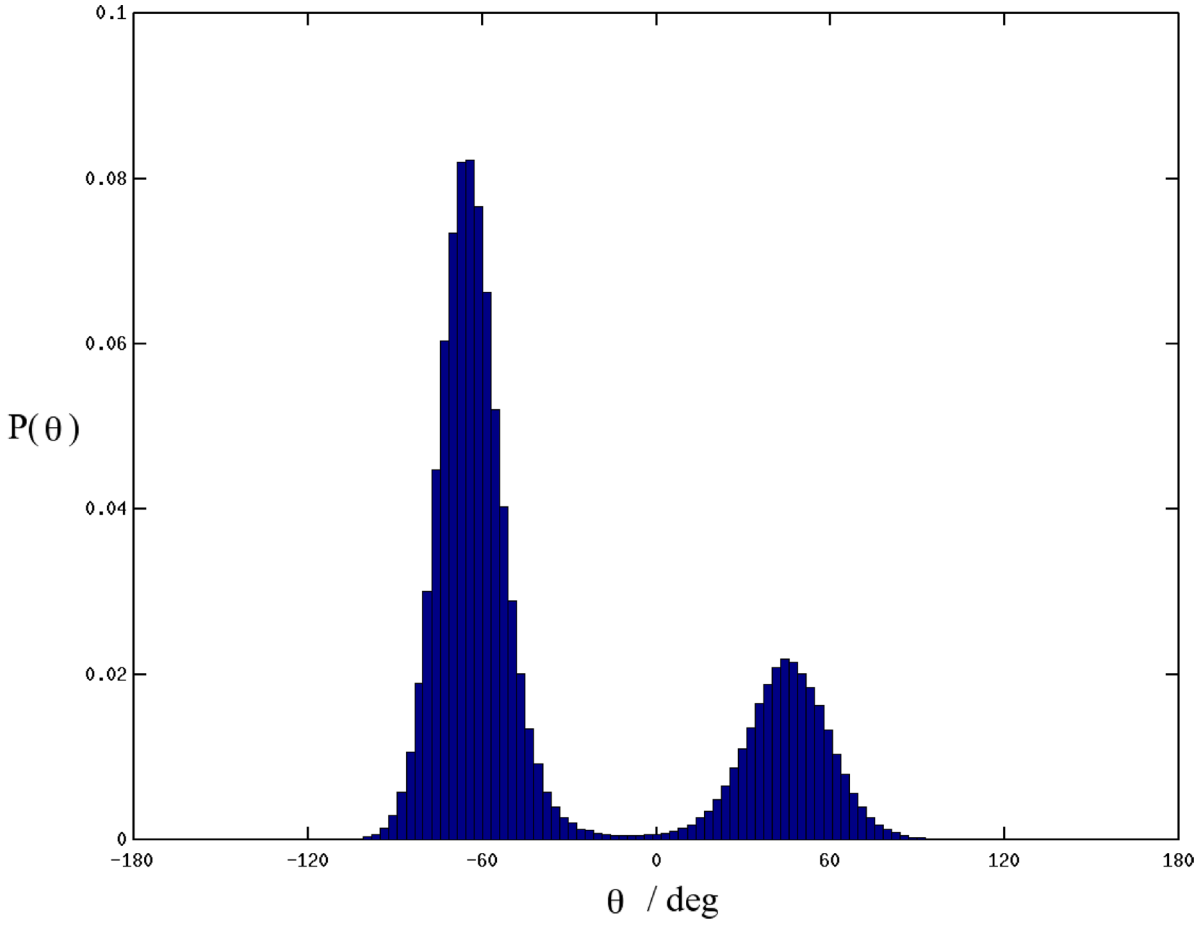

Figure 4. Histogram representation of equilibrium distribution of the torsional angle θ for one hydroxymethyl group of the γ-cyclodextrin obtained from the 200 ns MD trajectory.

acquired at higher temperatures, coefficients have been rescaled to the new temperature, T', as $c_k^2(T') = 300\ c_k^2(300\ \text{K})/T'$, giving $c_0^2(323\ \text{K}) = -13.22$, $c_2^2(323\ \text{K}) = -2.61$, and $c_0^2(343\ \text{K}) = -12.45$, $c_2^2(343\ \text{K}) = -2.47$. We assume that the potential parameters calculated in aqueous solution apply also in the mixed solvent D_2O/DMSO-d_6, used in the experimental work that we refer to below. A comparison and short discussion on the quality of the approximation of the potential of mean torque employed in the SRLS model (eq 4) to the MD-derived potential surface is given in the Supporting Information.

The global diffusion tensor has been evaluated using the DITE[28] software package with the following set of input parameters: $C = 6$ (stick boundary conditions), effective spheres radius $R = 2$ Å, temperature $T = 323$ and 343 K, viscosity of the 7:3 molar D_2O/DMSO-d_6 solution[39] $\eta = 2.9$ cP (at 323 K) and 2.3 cP (at 343 K). The time-independent reduced rotational tensor, i.e. the diffusion tensor scaled by the quantity $d_0 = k_BT/C\pi R\eta$, is $\mathbf{D}_1/d_0 = \text{diag}(2.6, 3.1, 3.2) \times 10^{-3}$ Å^{-2}. It shows very low anisotropy, which is not expected to affect sensibly the calculated NMR data, as shown in the Supporting Information. So, we assumed the rotational global motion to be isotropic, averaging the three principal components. As a result the rotational diffusion coefficients employed in the simulations are $D_1(323\ \text{K}) = 1.21 \times 10^8$ Hz and $D_1(343\ \text{K}) = 1.61 \times 10^8$ Hz. They correspond to correlation times of 1.4 and 1.0 ns, respectively. These results compare well, within 10% error, with correlation times determined earlier[14] of 1.6 and 0.9 ns, respectively. These correlation times have been determined by fitting the experimental NMR data with simple models based on the statistical independence of the global and internal motions. A discussion on the 10% variation of the global diffusion tensor on the quality of the fitting and the "propagation" of the uncertainty on the other model parameters is given in the Supporting Information. On the basis of our observations and simulations there is no sensible difference between the correlation times calculated with the hydrodynamic model and those obtained from the fitting of the experimental NMR data, confirming the (sufficient) quality of the HD method. To be consistent with our approach, based on the *a priori* evaluation of as most as possible model parameters, we use in our simulations the hydrodynamics-calculated global correlation times (global diffusion rates, to be precise).

The assumed orientation of the local ordering frame, OF, axes is shown on the Figure 3 (red color for X_{OF} axis, green for Y_{OF}, and blue color for Z_{OF}). Euler angles transforming from OF to dipolar frame of the first C−H bond (D_1F) were obtained from the reference structure (Figure 3). Here for 7 out of 8 units the $-CH_2OH$ group is in the predominant conformation ($\theta \approx -60$ deg). For that conformation (*conformation 1*) $\Omega_{OF\text{-}D1F} = (-145, 56, 106)$ deg. The last $-CH_2OH$ group is in the second conformation (*conformation 2* with $\theta \approx 60$ deg) with $\Omega_{OF\text{-}D2F} = (171, 136, 161)$ deg. Finally, the C−H bond length was fixed to 1.13 Å, which accounts for bond vibrations.[40,41]

dx.doi.org/10.1021/jp306624d | J. Phys. Chem. B 2012, 116, 13159−13171

A histogram analysis of the distribution of the θ angle from the MD trajectory revealed that conformation 1 is 4 times more probable than conformation 2 (see Figure 4). This analysis shows a continuous distribution of the torsional angle, while in the TS-SRLS model the motion is treated as a random walk between two discrete states. Thus, we set for conformation 1 ρ_1 = 0.8 and for conformation 2 ρ_2 = 0.2, such that their ratio is ρ_1/ρ_2 = 4, i.e., the ratio of two maxima of the distribution probability in Figure 4.

Calculation/fitting of NMR data has been carried out using the C^{2+}OPPS software package.[33,34] A single-point calculation with the truncation parameter L_{max} = 20 and isotropic global diffusion tensor took about 17 s on a Intel Core2 2.13 GHz laptop computer. The simulations, however, have been run on our cluster, parallelizing the calculation over 4 quad-core Intel Xeon 2.66 GHz CPU's (a total of 16 cores) connected via Infiniband. Each single-point step required 2 s and the full fitting, at the two temperatures, took a total of 3.5 h.

NMR data at both temperatures have been fitted using the principal values, $D_{2,\perp}$ and $D_{2,\parallel}$, of the (axial) local diffusion tensor, the two Euler angles $\alpha_{OF\text{-}M2F}$ and $\beta_{OF\text{-}M2F}$, giving its orientation on the probe, the jumping frequency, ω_R, and the planar angle H−C−H as free parameters. We decided to fit also the H−C−H, $\beta_{D1F\text{-}D2F}$, angle because NMR data, especially CCRRs, are extremely dependent on this angle and a sufficiently accurate computational estimation is not available. Fitting results for the parameters are shown in Table 2.

Table 2. TS-SRLS Model Parameters Obtained from Fitting of the NMR Data of γ-Cyclodextrin

T/K	$D_{2,\perp}/10^7$ Hz	$D_{2,\parallel}/10^{11}$ Hz	$\alpha_{OF\text{-}M_2F}$/ deg	$\beta_{OF\text{-}M_2F}$/ deg	$\beta_{D_1F\text{-}D_2F}$/ deg	$\omega_R/10^8$ Hz
323	5.6	2.5	−34.6	−29.5	111.1	5.0
343	17.9	8.1	−48.0	−40.1	111.9	4.3

Agreement with experimental relaxation data is very good, as shown in Table 3 and in Figures 5 and 6. Local diffusion tensors are shown in Table 2. The $D_{2,\perp}$ rate is close to the global rotational diffusion while the faster diffusion coefficient, $D_{2,\parallel}$, is 3 orders of magnitude larger. These are typical results expected for very rigid probes, as is the case of the α-glucopyranose unit, which feel a very high ordering. The results show that the motion associated with the twisting of the α-glucopyranose unit has the larger diffusion rate with respect to the other two rotations. The comparison with the recent paper by Bernatowicz et al.[19] is difficult because the models are quite different. Moreover, these authors reported measurements on ring carbons only while we concentrate here on the exocyclic CH_2 groups.

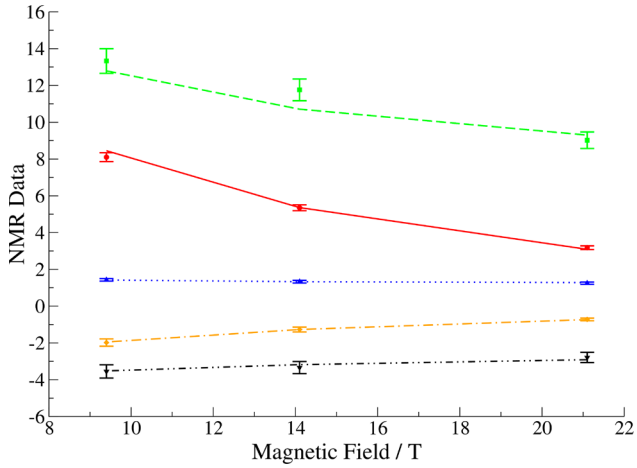

Figure 5. Calculated (lines) and experimental (points) NMR data of γ-cyclodextrin as a function of the magnetic field at 323 K: R_1 (red line/circles) in s^{-1}, R_2 (green dashed line/squares) in s^{-1}, NOE (blue dotted line/triangles up), Γ_{long} (orange dash dotted line/diamonds) in s^{-1}, and $\Gamma_{spin\text{-}lock}$ (black dash dot dotted line/triangles down).

The H−C−H planar angle obtained by fitting of NMR data is nearly temperature independent, in the range of temperatures taken into consideration, with an average value of 111.5 deg. As observed in similar systems[8] this value is larger than the tetrahedral value of 109.5 deg and may indicate the effect of internal motion.[41,42] As stated in section II, here we explicitly

Table 3. Comparison between Theoretical and Experimental NMR Data of γ-Cyclodextrin Obtained from Fitting at both 323 and 343 K[a]

		T = 323 K			T = 343 K		
	frequency/MHz	theor	expt	% diff	theor	expt	% diff
T_1/ms	400.0	120.4	123.5	−2.5	130.8	134.1	−2.4
T_2/ms		78.2	75.0	4.2	107.0	107.2	−0.2
NOE		1.45	1.43	1.4	1.689	1.630	3.6
CCRRT1/s^{-1}		−1.90	−1.98	−4.1	−1.535	−1.580	−2.8
CCRRT2/s^{-1}		−3.55	−3.55	0.0	−2.128	−2.160	−1.5
T_1/ms	600.0	186.6	187.0	−0.5	183.7	183.8	−0.1
T_2/ms		92.8	85.0	9.2	131.5	130.2	1.0
NOE		1.34	1.33	0.5	1.484	1.510	−1.7
CCRRT1/s^{-1}		−1.26	−1.27	−1.2	−1.190	−1.190	0.0
CCRRT2/s^{-1}		−3.22	−3.34	−3.5	−1.955	−1.870	4.6
T_1/ms	900.0	317.1	314.5	0.8	278.7	274.0	1.7
T_2/ms		106.5	110.9	−3.9	158.5	154.8	2.4
NOE		1.28	1.25	2.2	1.368	1.330	2.9
CCRRT1/s^{-1}		−0.73	−0.72	1.7	−0.804	−0.830	−3.1
CCRRT2/s^{-1}		−2.96	−2.79	6.2	−1.763	−1.710	3.1
red. χ^2		0.828			0.294		

[a]Reduced χ^2 is calculated as χ^2/ndf, with ndf =9 degrees of freedom (15 experimental points and 6 fitting parameters).

dx.doi.org/10.1021/jp306624d | J. Phys. Chem. B 2012, 116, 13159−13171

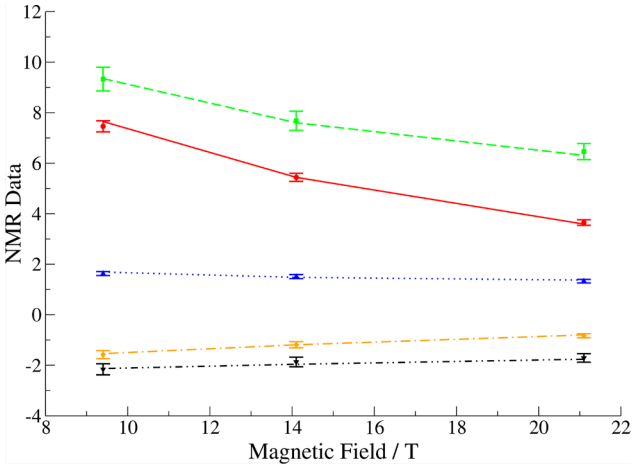

Figure 6. Calculated (lines) and experimental (points) NMR data of γ-cyclodextrin as a function of the magnetic field at 343 K: R_1 (red line/circles) in s^{-1}, R_2 (green dashed line/squares) in s^{-1}, *NOE* (blue dotted line/triangles up), Γ_{long} (orange dash dotted line/diamonds) in s^{-1}, and $\Gamma_{spin\text{-}lock}$ (black dash dot dotted line/triangles down).

neglected the H−C−H bond angle librations. However, as shown in Appendix B, it is possible to rigorously include this motion in the diffusive operator. We estimate that the fast libration influences calculated NMR data to an extent of about 1%. This is not affecting the quality of the agreement with experimental data, being the correction smaller than the experimental errors. However, it is worthy to note that the same 1% difference in the evaluated NMR data is obtained by neglecting the librational motion in the model and using a H−C−H bond angle 1−2 deg bigger than the expected value of 109.5 deg (see Appendix B). This observation justifies the H−C−H angle obtained from the fitting and confirms what is asserted in refs 41 and42.

Fitting of NMR data returns $\omega_R(323\ K) = 5.0 \times 10^8$ Hz and $\omega_R(343\ K) = 4.3 \times 10^8$ Hz. The frequency is nearly temperature independent. However, a small dependence is observed with the frequency being smaller at 343 K. This seems counterintuitive and it must be underlined that ω_R does not count the number of jumps between the two sites in the unit time, rather it is related to the relaxation of the stochastic process. At higher temperature a larger number of jumps is expected to occur between the two states, thus relaxation of the stochastic process is expected to occur with a larger time-scale, i.e., with a smaller ω_R. We shall notice that the fitted jump frequency is also in reasonable agreement with the values reported by Ghalebani et al.,[14] based on the interpretation of the same NMR relaxation data using simpler dynamic model, and with the results of ultrasonic relaxation studies.[43,44]

A comment is necessary concerning the fitting procedure. The existence of multiple minima in the χ^2 function is one of the most problematic issues that can rise, in general, in the application of nonlinear least-squares fitting procedures for the determination of unknown physical model parameters and SRLS is not exempt from this problem. The danger is 2-fold. First, the search algorithm can land and get stuck on a local minimum of the χ^2 surface and second this local minimum can correspond to a set of physically unacceptable parameters. The problem is how to determine if the fitting parameters are physically acceptable when we use a fitting scheme because we are not able to predict/calculate them. The best scenario would be the one in which all the model parameters can be calculated *a priori*. In our simulations we were able to determine 75% of the model parameters. Unfortunately this means that six parameters were still free. For two of these parameters, namely the H−C−H bond angle and the hydroxymethyl jump rate, we should expect a value around 109.5 deg for the former, based on quantum mechanical calculations, and around 10^9 Hz for the latter, based on the observations of other researchers. Considerations on the local diffusion tensor (with regards to both the principal values and the orientation) are much more difficult given the complexity of the physical nature of this molecular parameter. On the basis of previous applications of the SRLS model to interpret NMR data we observed that in highly ordered situations the anisotropy of the local diffusion tensor $D_{2,\|}/D_{2,\perp}$ is usually very large and the $D_{2,\perp}$ is usually of the same order of the global diffusion tensor. Thus, based on all these observations we set up a probably good initial guess. As discussed before, the obtained model parameters are in agreement with findings of other authors and, to us, the global physical picture is solid. Together with the good agreement between calculated and experimental NMR data we shall assert that the fitting landed in an acceptable minimum of the χ^2 surface.

The integrated computational approach presented in this work determines an operative protocol that can be applied to similar systems for which the description of local dynamics in terms of usual internal coordinates is not possible because too many coordinates need to be included and/or complex generalized coordinates, as the ring-coordinate in the case of cyclodextrins, should be employed. When treating molecular systems much different from cyclodextrins one should follow the full protocol, i.e.: MD simulations to get the potential surfaces, HD calculations for the global diffusion tensor, and stochastic simulations to get the NMR data. However, we conjecture that for related cyclodextrins it is possible to omit the MD step and employ directly the potential surfaces calculated for the studied γ-cyclodextrin. This is expected because due to the closed ring geometry it is reasonable to assume that the glucopyranose units will be characterized by very similar local ordering. The application of the method to the simulation of NMR data of an α-cyclodextrin (data reported in the Supporting Information) confirmed the hypothesis. Thus, by induction we state that, as first approximation, the family of cyclodextrins can be parametrized, in the calculation of NMR observables, with the MD-derived potential energy surface used in this work for the γ-cyclodextrin. A more careful and systematic study is in progress to confirm these conjectures.

IV. CONCLUSIONS

Results presented in section III show that the TS-SRLS model is able to describe the relevant dynamic processes linked to NMR relaxation data in the case of γ-cyclodextrin. The method provides a relatively simple approach to a rationalization of closed ring geometries in which local dynamics is too complicated to be described using standard internal coordinates (i.e., bond lengths, bond angles and torsional angles). In the case of cyclodextrins the internal dynamics could be described using appropriate ring generalized coordinates. In this case leaving the atomistic detail in favor of a more coarse-grained view allows to maintain, at a relatively simple level, the description of the coupling of local (internal) motion with the global (reorientational) motion of the system within an

augmented two-body model, leading to a good agreement with experimental data.

APPENDIX A. SPECTRAL DENSITIES OF THE TS-SRLS MODEL

In this Appendix, we discuss in more detailed way the treatment of the random walk operator and the calculation of spectral densities for the TS-SRLS model. We recall that the stochastic process is $\mathbf{Q} = (\Omega_{\text{LF-VF}},\Omega_{\text{VF-OF}},\theta) = (\mathbf{Y},\theta)$, with $\mathbf{Y}$ collecting the two sets of Euler angles giving the orientations of the two bodies and θ being the internal generalized coordinate that describes the orientation of the hydroxymethyl group on the probe (second body). We shall write the Smoluchowski operator as

$$\hat{\Gamma}(\mathbf{Q}) = \hat{\Gamma}_{SRLS}(\mathbf{Y}) + \hat{\Gamma}_{RW}(\mathbf{Q}) \tag{A1}$$

where $\hat{\Gamma}_{SRLS}$ is the "standard" SRLS diffusive operator,[10] while the random walk operator is defined by the following master equation

$$\hat{\Gamma}_{RW}P(\mathbf{Q}, t) = \int d\mathbf{Q}' \,[P(\mathbf{Q}, t)W(\mathbf{Q} \rightarrow \mathbf{Q}') - P(\mathbf{Q}', t)W(\mathbf{Q}' \rightarrow \mathbf{Q})] \tag{A2}$$

where $P(\mathbf{Q},t)$ is the probability density of finding the system in configuration $\mathbf{Q}$ at time t if it was in configuration $\mathbf{Q}_0$ at time $t_0 = 0$, and $W(\mathbf{Q}\rightarrow\mathbf{Q}')$ is the kernel of the transformation between configurations $\mathbf{Q}$ and $\mathbf{Q}'$. As underlined in section II.A, we make the following assumptions: (*i*) a change in the value of the internal coordinate θ does not influence the orientation of the two bodies, (*ii*) the potential of mean force is decoupled in a term depending only on the rotational coordinates of the two bodies and a term that depends only on the internal coordinate, and (*iii*) the rate of the transition between different states of θ is independent of the configuration of the system. On the basis of these premises, the kernel of the transformation can be straightforwardly written as

$$W(\mathbf{Q} \rightarrow \mathbf{Q}') = \omega_R\delta(\mathbf{Y} - \mathbf{Y}')P_{eq}(\theta') \tag{A3}$$

where ω_R is the jumping frequency between different values of θ. Substitution of the kernel defined in eq A3 into the master equation reads

$$\hat{\Gamma}_{RW}P(\mathbf{Q}, t) = \omega_R[P(\mathbf{Q}, t) - P_{eq}(\theta)] \tag{A4}$$

By introducing the symmetrization of the Smoluchowski operator $\tilde{\Gamma} = P_{eq}^{-1/2}(\mathbf{Q})\hat{\Gamma}P_{eq}^{1/2}(\mathbf{Q})$ and the symmetrized probability density $\tilde{P}(\mathbf{Q}, t) = P_{eq}^{-1/2}(\mathbf{Q})P(\mathbf{Q}, t)$ the random walk operator in eq A4 changes to

$$\tilde{\Gamma}_R\tilde{P}(\mathbf{Q}, t) = \omega_R[1 - P_{eq}^{1/2}(\theta) \int dq' \, P_{eq}^{1/2}(\theta')\cdot]\tilde{P}(\mathbf{Q}, t) \tag{A5}$$

In the specific case of the jump motion of the hydroxymethyl group the coordinate θ is discretized over two states $|n\rangle = \{|1\rangle,|2\rangle\}$ that simply select the value of θ, i.e. $|n\rangle = \delta(\theta - \theta n)$. This basis is orthonormal, since

$$\langle n|n'\rangle = \int dq \, \delta(\theta - \theta_n)\delta(\theta - \theta_{n'}) = \delta(\theta_n - \theta_{n'}) \tag{A6}$$

The full Smoluchowski operator is spanned over the set of basis functions $|\Lambda\rangle = |\lambda\rangle \otimes |n\rangle$, where $|\lambda\rangle = |L_1M_1K_1,L_2M_2K_2\rangle$ is the standard SRLS basis set of Wigner matrices. The matrix elements of the Smoluchowski operator are

$$\langle\Lambda|\tilde{\Gamma}|\Lambda'\rangle = \delta_{n,n'}(\Gamma_0)_{\lambda,\lambda'} + \delta_{\lambda,\lambda'}\omega_R(\delta_{n,n'} - \sqrt{\rho_1\rho_2}) \tag{A7}$$

where $(\mathbf{\Gamma}_0)\lambda,\lambda'$ are the SRLS matrix elements and we introduced the notation $\rho_i = P_{eq}(\theta)_{|q=qi}$. We shall notice here that we can span the symmetrized equilibrium probability density of coordinate θ as $P_{eq}^{1/2}(\theta) = \rho_1^{1/2}\delta(\theta - \theta_1) + \rho_2^{1/2}\delta(\theta - \theta_2) = \rho_1^{1/2}|1\rangle + \rho_2^{1/2}|2\rangle$.

It is convenient to use the following linear combinations of states $|n\rangle$

$$\begin{cases} |+\rangle = \rho_1^{1/2}|1\rangle + \rho_2^{1/2}|2\rangle \\ |-\rangle = \rho_2^{1/2}|1\rangle - \rho_2^{1/2}|2\rangle \end{cases} \tag{A8}$$

This is still an orthonormal basis

$$\langle+|+\rangle = \langle\rho_1^{1/2}\delta(\theta - \theta_1) + \rho_2^{1/2}\delta(\theta - \theta_2)|\rho_1^{1/2}\delta(\theta - \theta_1) + \rho_2^{1/2}\delta(\theta - \theta_2)\rangle = \rho_1 + \rho_2 = 1 \tag{A9a}$$

$$\langle-|-\rangle = \langle\rho_2^{1/2}\delta(\theta - \theta_1) - \rho_1^{1/2}\delta(\theta - \theta_2)|\rho_2^{1/2}\delta(\theta - \theta_1) - \rho_1^{1/2}\delta(\theta - \theta_2)\rangle = \rho_2 + \rho_1 = 1 \tag{A9b}$$

$$\langle+|-\rangle = \langle\rho_1^{1/2}\delta(\theta - \theta_1) + \rho_2^{1/2}\delta(\theta - \theta_2)|\rho_2^{1/2}\delta(\theta - \theta_1) - \rho_2^{1/2}\delta(\theta - \theta_2)\rangle = 0 \tag{A9c}$$

Furthermore, the two states $|\pm\rangle$ are eigenfunctions of the Smoluchowski operator. To prove the latter statement we shall first notice that $P_{eq}^{1/2}(\theta) = |\pm\rangle$. Using this fact, one can write

$$\tilde{\Gamma}|+\rangle = \tilde{\Gamma}_{SRLS}|+\rangle + \omega_R[|+\rangle - |+\rangle\langle+|+\rangle] = \tilde{\Gamma}_{SRLS}|+\rangle \tag{A10a}$$

$$\tilde{\Gamma}|-\rangle = \tilde{\Gamma}_{SRLS}|-\rangle + \omega_R[|-\rangle - |+\rangle\langle+|-\rangle] = (\tilde{\Gamma}_{SRLS} + \omega_R)|-\rangle \tag{A10b}$$

The following correlation functions are required to access NMR relaxation data

$$\begin{aligned} C^{\mu\nu}(t) &\propto \langle D_{0,0}^{2}(\Omega_{L\mu}(\mathbf{Q}))P_{eq}^{1/2}(\mathbf{Q})|e^{-\tilde{\Gamma}t}|D_{0,0}^{2}(\Omega_{L\nu}(\mathbf{Q}))P_{eq}^{1/2}(\mathbf{Q})\rangle \\ &= \sum_{K,K'} \langle D_{K,0}^{2}(\Omega_{\text{OF-}\mu\text{F}}(\theta))D_{0,K}^{2}(\mathbf{Y})P_{eq}^{1/2}(\mathbf{Q})|e^{-\tilde{\Gamma}t}| \\ &\quad D_{K',0}^{2}(\Omega_{\text{OF-}\nu\text{F}}(\theta))D_{0,K'}^{2}(\mathbf{Y})P_{eq}^{1/2}(\mathbf{Q})\rangle \\ &= \sum_{K,K'} C_{KK'}^{\mu\nu}(t) \end{aligned} \tag{A11}$$

It is convenient to use the closure relation of the subset of functions $\{|+\rangle,|-\rangle\}$ in the correlation functions appearing in the summation in the second equality of eq A11

dx.doi.org/10.1021/jp306624d | J. Phys. Chem. B 2012, 116, 13159−13171

$$C^{\mu\nu}_{KK'}(t) = \sum_{n,n'=\pm} \langle {D_{K,0}}^2(\Omega_{\text{OF-}\mu\text{F}}(\theta)) {P_{eq}}^{1/2}(\theta)|n\rangle\langle n'| {D_{K',0}}^2(\Omega_{\text{OF-}\nu\text{F}}(\theta)) {P_{eq}}^{1/2}(\theta)\rangle \times \langle {D_{0,K}}^2(\mathbf{Y}) {P_{eq}}^{1/2}(\mathbf{Y})\langle n|e^{-\tilde{\Gamma}t}|n'\rangle {D_{0,K'}}^2(\mathbf{Y}) {P_{eq}}^{1/2}(\mathbf{Y})\rangle$$
$$= \chi^{+*}_{\mu,K}\chi^{+}_{\nu,K'}\langle {D_{0,K}}^2(\mathbf{Y}) {P_{eq}}^{1/2}(\mathbf{Y})|e^{-\tilde{\Gamma}_{SRLS}t}|{D_{0,K'}}^2(\mathbf{Y}) {P_{eq}}^{1/2}(\mathbf{Y})\rangle + \chi^{-*}_{\mu,K}\chi^{-}_{\nu,K'}\langle {D_{0,K}}^2(\mathbf{Y}) {P_{eq}}^{1/2}(\mathbf{Y})|e^{-(\tilde{\Gamma}_{SRLS}+\omega_R)t}|{D_{0,K'}}^2(\mathbf{Y}) {P_{eq}}^{1/2}(\mathbf{Y})\rangle \tag{A12}$$

where

$$\chi^{+}_{\mu,K} = \rho_1 {D_{K,0}}^2(\Omega_{\mu,1}) + \rho_2 {D_{K,0}}^2(\Omega_{\mu,2}) \tag{A13a}$$

$$\chi^{-}_{\mu,K} = \sqrt{\rho_1\rho_2}\,{D_{K,0}}^2(\Omega_{\mu,1}) - \sqrt{\rho_1\rho_2}\,{D_{K,0}}^2(\Omega_{\mu,2}) \tag{A13b}$$

and $\Omega_{\mu,i} = \Omega_{\text{OF-}\mu\text{F}}(\theta)_{|\theta=\theta i}$. The spectral density is obtained by taking the real part of the Fourier-Laplace transform of eq A11

$$J^{\mu,\nu}(\omega) = \sum_{K,K'} \text{Re}\{\chi^{+*}_{\mu,K}\chi^{+}_{\nu,K'}\} j^{+}_{K,K'}(\omega) + \text{Re}\{\chi^{-*}_{\mu,K}\chi^{-}_{\nu,K'}\} j^{-}_{K,K'}(\omega) \tag{A14}$$

where the $j^{+}_{K,K'}(\omega)$ functions correspond exactly to the standard SRLS spectral densities, while the $j^{-}_{K,K'}(\omega)$ functions are the SRLS spectral densities calculated with an intrinsic line width corresponding to ω_R.

APPENDIX B. MODELING OF THE H−C−H LIBRATION

In order to include the fast libration of the H−C−H angle, β_{HCH}, of the hydroxymethyl group one needs to add to the SRLS operator a term describing the relaxation of the new stochastic coordinate. The simplest choice in case of a libration is to consider this motion as decoupled from the other coordinates, which means that (*i*) no hydrodynamic coupling is accounted for in the diffusion tensor and (*ii*) the potential of mean force is the sum of two contributions, i.e., $U(\Omega_{\text{VF-OF}},\beta_{HCH}) = U_{SRLS}(\Omega_{\text{VF-OF}}) + U_{HCH}(\beta_{HCH})$. In this case, the full diffusive operator reads

$$\hat{\Gamma}(\Omega_{\text{LF-VF}}, \Omega_{\text{VF-OF}}, \beta_{HCH}) = \hat{\Gamma}_{SRLS}(\Omega_{\text{LF-VF}}, \Omega_{\text{VF-OF}}) - d\frac{\partial}{\partial\beta_{HCH}} P_{eq}(\beta_{HCH}) \frac{\partial}{\partial\beta_{HCH}} {P_{eq}}^{-1}(\beta_{HCH})$$
$$= \hat{\Gamma}_{SRLS}(\Omega_{\text{LF-VF}}, \Omega_{\text{VF-OF}}) + \hat{\Gamma}_{HCH}(\beta_{HCH}) \tag{B1}$$

where $\hat{\Gamma}_{SRLS}$ is defined in eq 2, d is the diffusion coefficient for the H−C−H libration and the equilibrium distribution is the Maxwell probability density

$$P_{eq}(\beta_{HCH}) = \exp[-U_{HCH}(\beta_{HCH})/k_B T]/Z \tag{B2}$$

Z being the (reduced) partition function.

We approximate the potential of mean force as being harmonic

$$U_{HCH}(\beta_{HCH}) = \frac{1}{2}k(\beta_{HCH} - \beta^0_{HCH})^2 \tag{B3}$$

where β^0_{HCH} is the bond angle corresponding to the minimum energy configuration. The partition function is

$$Z = \int_0^\pi d\beta_{HCH}\, \sin(\beta_{HCH}) e^{-1/2k(\beta_{HCH}-\beta^0_{HCH})^2} = \int_{-\beta^0_{HCH}}^{\pi-\beta^0_{HCH}} dy\, [s_0\cos(y) + c_0\sin(y)] e^{-1/2ky2} \tag{B4}$$

where $s_0 = \sin(\beta^0_{HCH})$, $c_0 = \cos(\beta^0_{HCH})$, and $y = \beta_{HCH} - \beta^0_{HCH}$. It is reasonable to assume, for a libration, that $k \gg 1$. In this limit we can approximate $\sin(y) \approx y$ and $\cos(y) \approx 1 - y^2/2$, and extend to $\pm\infty$ the integration extremes. Thus, the partition function reads

$$Z \approx s_0 \int_{-\infty}^{+\infty} dy \left(1 - \frac{1}{2}y^2\right) e^{-(1/2)ky2} = s_0\sqrt{\frac{2\pi}{k}}\left(1 - \frac{1}{2k}\right) \approx s_0\sqrt{\frac{2\pi}{k}} \tag{B5}$$

We now evaluate the effect of the H−C−H libration on the dipolar−dipolar cross-correlation. Analogous considerations can be straightforwardly done on the dipolar autocorrelations. The physical observable is defined as the cross-correlation function $C^{D_1,D_2}(t)$ defined as

$$C^{D_1,D_2}(t) \propto \langle {D_{0,0}}^{2*}(\Omega_{\text{LF-}D_1\text{F}}(0)) {D_{0,0}}^2(\Omega_{\text{LF-}D_2\text{F}}(t))\rangle = \sum_{K,K',M=-2}^{2} {D_{K,0}}^{2*}(\Omega_{\text{OF-}D_1\text{F}}) {D_{K',M}}^2(\Omega_{\text{OF-}D_1\text{F}}) \times \int d\mathbf{X}\, {D_{0,K}}^{2*}(\Omega_{\text{LF-OF}}) e^{-\hat{\Gamma}t} {D_{0,K'}}^2(\Omega_{\text{LF-OF}}) {d_{M,0}}^2(\beta_{HCH}) P_{eq}(\Omega_{\text{OF-VF}}, \beta_{HCH}) \tag{B6}$$

where $d\mathbf{X} = d\Omega_{\text{LF-VF}}\, d\Omega_{\text{VF-OF}}\, d\beta_{HCH}\, \sin(\beta_{HCH})$. The two terms in the diffusive operator in eq B1 commute, so the integral in the last equality of eq B6 is factorized in the two terms

$$c^{(SRLS)}_{K,K'}(t) = \int d\Omega_{\text{LF-VF}}\, d\Omega_{\text{VF-OF}}\, {D_{0,K}}^{2*}(\Omega_{\text{LF-OF}}) e^{-\hat{\Gamma}_{SRLS}t} {D_{0,K'}}^2(\Omega_{\text{LF-OF}}) P_{eq}(\Omega_{\text{LF-OF}}) \tag{B7}$$

which are the standard SRLS reduced correlation functions, and

$$c^{(HCH)}_{M}(t) = \int d\beta_{HCH}\, \sin(\beta_{HCH}) e^{-\hat{\Gamma}_{HCH}t} {d_{M,0}}^2(\beta_{HCH}) P_{eq}(\beta_{HCH}) \tag{B8}$$

Notice that while the reduced correlation functions (the small $c(t)$ functions) are factorized, the total correlation function, $C^{D_1,D_2}(t)$, is not because a coupling of the different kinds of motion is imposed by the physical observable.

To evaluate the $c^{(HCH)}_M(t)$ functions we first expand the reduced Wigner matrices around the equilibrium value (i.e., around $y = 0$) stopping at the second order

dx.doi.org/10.1021/jp306624d | J. Phys. Chem. B 2012, 116, 13159−13171

$$d_{0,0}{}^2(y) \approx d_{0,0}{}^2(\beta^0_{HCH}) - 3c_0s_0y - \frac{3}{2}(1 - s_0{}^2)y^2 \quad \text{(B9)}$$

$$d_{1,0}{}^2(y) \approx d_{1,0}{}^2(\beta^0_{HCH}) - \sqrt{\frac{3}{2}}(1 - 2s_0{}^2)y + \sqrt{6}\,c_0s_0y^2 \quad \text{(B10)}$$

$$d_{2,0}{}^2(y) \approx d_{2,0}{}^2(\beta^0_{HCH}) + \sqrt{\frac{3}{2}}\,c_0s_0y + \sqrt{\frac{3}{8}}(1 - 2s_0{}^2)y^2 \quad \text{(B11)}$$

All the reduced Wigner matrices, thus, take the general form $d_{M,0}{}^2(y) \approx d_{M,0}{}^2(\beta^0_{HCH}) + a_My + b_My^2$. Next, we shall evaluate the effect of the exponential operator $\exp(-\hat{\Gamma}_{HCH}t)$ over $d_{M,0}{}^2(y)P_{eq}(y)$. With some cumbersome passages one gets

$$e^{-\hat{\Gamma}_{HCH}t}d_{M,0}{}^2(y)P_{eq}(y) \approx \left[d_{M,0}{}^2(\beta^0_{HCH}) + a_Me^{-k\,dt}y + b_M\left(y^2 - \frac{1}{k}\right)e^{-2k\,dt}\right] P_{eq}(y) \quad \text{(B12)}$$

Substitution of eq B12 into eq B8 and integrating using the same assumptions done in the calculation of the partition function, the approximate form of $c_M^{(HCH)}(t)$ reads

$$c_M^{(HCH)}(t) \approx \left(1 - \frac{1}{2k}\right)d_{M,0}{}^2(\beta^0_{HCH}) + \frac{1}{k}\frac{c_0}{s_0}a_Me^{-k\,dt} \quad \text{(B13)}$$

which was obtained neglecting terms containing $1/k^n$ with $n > 1$. In the further assumption of very large diffusion coefficient, $d \gg 10^9$ Hz, the last term in eq B13 can be neglected, thus neglecting the "dynamic" effect the H−C−H libration, i.e. it is reasonable to consider that the β_{HCH} angle is at equilibrium while the other stochastic variables are relaxing. Thus, only an average effect (vibrational averaging) survives in the reduced correlation function

$$c_M^{(HCH)}(t) \approx \left(1 - \frac{1}{2k}\right)d_{M,0}{}^2(\beta^0_{HCH}) \quad \text{(B14)}$$

and the total cross-correlation function reads

$$C^{D_1,D_2}(t) \approx \left(1 - \frac{1}{2k}\right)C^{D_1,D_2}_{SRLS}(t|\beta_{HCH})_{|\beta_{HCH}=\beta^0_{HCH}} \quad \text{(B15)}$$

From the MD trajectory we evaluated k being on the order of 10^2, thus the correction to the total cross-correlation function is around 1%. From the point of view of the agreement with the experimental data, such a correction is smaller than the usual experimental errors. Thus, a 1% correction to the theoretical NMR data is not sensibly affecting the overall agreement, expressed in terms of the reduced χ^2. However, in this case it is noteworthy to consider the effect of this correction on the estimation, via fitting, of the β_{HCH} angle. We shall define the vibrationally averaged quantity

$$C^{D_1,D_2}(t) = \overline{C^{D_1,D_2}_{SRLS}(t|\beta_{HCH})} \approx \left(1 - \frac{1}{2k}\right)C^{D_1,D_2}_{SRLS}(t|\beta^0_{HCH}) = C^{D_1,D_2}_{SRLS}(t|\beta^{eff}_{HCH}) \quad \text{(B16)}$$

where β^{eff}_{HCH} is some effective bond angle such that the calculation of the correlation function at the fixed value β^{eff}_{HCH} corresponds to the vibrationally averaged correlation function evaluated with the correct H−C−H angle, β^0_{HCH}. The same 1% difference in the observed NMR data obtained from the averaging of the correlation functions is obtained calculating the "single-point" correlation function, $C^{D_1,D_2}_{SRLS}(t|\beta^{eff}_{HCH})$, with a β^{eff}_{HCH} about 1.5−2 deg larger than β^0_{HCH}. E.g., the CCRRT's at 400 MHz and 323 K without the vibrational correction evaluated for β_{HCH} = 109.5 deg are CCRRT1 = −2.101 Hz and CCRRT2 = −3.786 Hz, while their values calculated at β_{HCH} = 111.1 deg are CCRRT1 = −1.948 Hz and CCRRT2 = −3.522 Hz. This explains why in our fitting we find an average β_{HCH} angle of 111.5 deg, while the expected value is 109.5 deg.

■ ASSOCIATED CONTENT

Supporting Information

Effect of coupling among motions, potential of mean torque, global diffusion anisotropy, global correlation time, and application to α-cyclodextrin. This material is available free of charge via the Internet at http://pubs.acs.org.

■ AUTHOR INFORMATION

Corresponding Author

*E-mail: antonino.polimeno@unipd.it. Telephone: (+39) 049 8275146. Fax: (+39) 049 8275829.

Notes

The authors declare no competing financial interest.

■ ACKNOWLEDGMENTS

This work was supported by Ministero dell'Istruzione, Università e Ricerca (MIUR), Grant PRIN Time 2008, by the University of Padova, Grant "Progetto Strategico" Helios 2009, and by the CMST COST Action CM1002 "CODECS". Support from the Swedish Research Council (Contracts 621-2010-4890 and 621-2011-3311) is gratefully acknowledged.

■ REFERENCES

(1) Cavanagh, J.; Fairbrother, W. J.; Palmer, A. G.; Skelton, N. J. *Protein NMR Spectroscopy*; Academic: San Diego, CA, 1996.
(2) Landersjö, C.; Stenutz, R.; Widmalm, G. *J. Am. Chem. Soc.* **1997**, *119*, 8695.
(3) Kowalewski, J.; Mäler, L. *Nuclear Spin Relaxation in Liquids*; Taylor & Francis: New York, 2006.
(4) Murali, N.; Krishnan, V. V. *Conc. Magn. Reson. A* **2003**, *17A*, 86.
(5) Tolman, J. R.; Ruan, K. *Chem. Rev.* **2006**, *106*, 1720.
(6) Meirovitch, E.; Shapiro, Y. E.; Polimeno, A.; Freed, J. H. *J. Phys. Chem. A* **2006**, *110*, 8366.
(7) Meirovitch, E.; Shapiro, Y. E.; Polimeno, A.; Freed, J. H. *Prog. NMR Spectrosc.* **2010**, *56*, 360.
(8) Zerbetto, M.; Polimeno, A.; Kotsyubynskyy, D.; Ghalebani, L.; Kowalewski, J.; Meirovitch, E.; Olsson, U.; Widmalm, G. *J. Chem. Phys.* **2009**, *131*, 234501.
(9) Zerbetto, M.; Buck, M.; Meirovitch, E.; Polimeno, A. *J. Phys. Chem. B* **2011**, *115*, 376.
(10) Polimeno, A.; Freed, J. H. *J. Phys. Chem.* **1995**, *99*, 10995.
(11) Shapiro, Y. E.; Polimeno, A.; Freed, J. H.; Meirovitch, E. *J. Phys. Chem. B* **2011**, *115*, 354.
(12) Meirovitch, E.; Zerbetto, M.; Polimeno, A.; Freed, J. H. *J. Phys. Chem. B* **2011**, *115*, 143.
(13) Meirovitch, E.; Shapiro, Y. E.; Zerbetto, M.; Polimeno, A. *J. Phys. Chem. B* **2012**, *116*, 886.
(14) Ghalebani, L.; Kotsyubynskyy, D.; Kowalewski, J. *J. Magn. Reson.* **2008**, *195*, 1.
(15) Kowalewski, J.; Widmalm, G. *J. Phys. Chem.* **1994**, *98*, 28.
(16) Lipari, G.; Szabo, A. *J. Am. Chem. Soc.* **1982**, *104*, 4546.
(17) Lipari, G.; Szabo, A. *J. Am. Chem. Soc.* **1982**, *104*, 4559.

(18) Daragan, V. A.; Mayo, K. H. *Prog. NMR Spectrosc.* **1997**, *31*, 63.
(19) Bernatowicz, P.; Ruszczynska-Bartnik, K.; Ejchart, A.; Dodziuk, H.; Kaczorowska, E.; Ueda, H. *J. Phys. Chem. B* **2010**, *114*, 59.
(20) Bernatowicz, P.; Kowalewski, J.; Szymanski, S. *J. Chem. Phys.* **2006**, *124*, 024108.
(21) Behrends, R.; Kaatze, U. *Chem. Phys. Chem.* **2005**, *6*, 1133.
(22) Kaminski, K.; Wlodarczyk, P.; Adrjanowicz, K.; Kaminska, E.; Wojnarowska, Z.; Paluch, M. *J. Phys. Chem. B* **2010**, *114*, 11272.
(23) Zhang, Z.; Fleissner, M. R.; Tipikin, D. S.; Liang, Z.; Moscicki, J. K.; Earle, K. A.; Hubbell, W. L.; Freed, J. H. *J. Phys. Chem. B* **2010**, *114*, 5503.
(24) Polnaszek, C. F.; Freed, J. H. *J. Phys. Chem.* **1975**, *21*, 2283.
(25) Stenutz, R.; Carmichael, I.; Widmalm, G.; Serianni, A. S. *J. Org. Chem.* **2002**, *67*, 949.
(26) (a) Bloomfield, V. A.; Dalton., W. G.; Van Holde, K. E. *Biopolymers* **1967**, *5*, 135. (b) Bloomfield, V. A. *Science* **1968**, *161*, 1212.
(27) (a) De La Torre, J. G.; Bloomfield, V. A. *Rev. Biophys.* **1981**, *14*, 81. (b) De La Torre, J. G.; Huertas, M. L.; Carrasco, B. *J. Magn. Reson.* **2000**, *147*, 138.
(28) Barone, V.; Zerbetto, M.; Polimeno, A. *J. Comput. Chem.* **2009**, *30*, 2.
(29) Moro, G. *Chem. Phys.* **1987**, *118*, 181.
(30) Moro, G. J.; Freed, J. H. *Large-Scale Eigenvalue Problems, Math Studies Series*; Cullum, J., Willough, R.; Eds.; North Holland: Amsterdam, 1986; Vol. *127*, p 143.
(31) Chen, Y. Y.; Luo, S. Y.; Hung, S. C.; Chan, S. I.; Tzou, D. L. M. *Carbohydr. Res.* **2005**, *340*, 723.
(32) Abragam, A. *The Principles of Nuclear Magnetism*: Oxford University Press (Clarendon): Oxford, U.K., 1961.
(33) Zerbetto, M.; Polimeno, A.; Meirovitch, E. *J. Phys. Chem. B* **2009**, *113*, 13613.
(34) Zerbetto, M.; Polimeno, A.; Meirovitch, E. *Int. J. Quantum Chem.* **2010**, *110*, 387.
(35) Moro, G. J.; Freed, J. H. *J. Chem. Phys.* **1981**, *74*, 3757.
(36) Phillips, J. C.; Braun, R.; Wang, W.; Gumbart, J.; Tajkhorshid, E.; Villa, E.; Chipot, C.; Skeel, R. D.; Kale, L.; Schulten., K. *J. Comput. Chem.* **2005**, *26*, 1781.
(37) Kuttel, M.; Brady, J. W.; Naidoo, K. J. *J. Comput. Chem.* **2000**, *23*, 1236.
(38) Brooks, B. R.; Bruccoleri, R. E.; Olafson, B. D.; States, D. J.; Swaminathan, S.; Karplus, M. *J. Comput. Chem.* **1983**, *4*, 187.
(39) Schichman, S. A.; Amey, R. L. *J. Phys. Chem.* **1971**, *75*, 98.
(40) Henry, E. R.; Szabo, A. *J. Chem. Phys.* **1985**, *82*, 4753.
(41) Kowalewski, J.; Effemey, M.; Jokisaari, J. *J. Magn. Reson.* **2002**, *157*, 171.
(42) Ghalebani, L.; Bernatowicz, P.; Aski, S. N.; Kowalewski, J. *Concepts Magn. Reson. A* **2007**, *30*, 100.
(43) Behrends, R.; Cowman, M. K.; Eggers, F.; Eyring, E. M.; Kaatze, U.; Majewski, J.; Petrucci, S.; Richmann, K.-H.; Riech, M. *J. Am. Chem. Soc.* **1997**, *119*, 2182.
(44) Stenger, J.; Cowman, M.; Eggers, F.; Eyring, E. M.; Kaatze, U.; Petrucci, S. *J. Phys. Chem. B* **2000**, *104*, 4782.